



Continuous electrochemical treatment of simulated industrial textile wastewater from industrial components in a tubular reactor

Bahadır K. Körbahti^a, Abdurrahman Tanyolaç^{b,*}

^a Faculty of Engineering, Department of Chemical Engineering, University of Mersin, Çiftlikköy, 33343 Mersin, Turkey

^b Faculty of Engineering, Department of Chemical Engineering, Hacettepe University, Beytepe, 06800 Ankara, Turkey

ARTICLE INFO

Article history:

Received 7 October 2008

Received in revised form 7 May 2009

Accepted 8 May 2009

Available online 18 May 2009

Keywords:

Electrochemical wastewater treatment

Textile wastewater

Tubular reactor

Mass transfer

Energy consumption

ABSTRACT

The continuous electrochemical treatment of industrial textile wastewater in a tubular reactor was investigated. The synthetic wastewater was based on the real process information of pretreatment and dyeing stages of the industrial mercerized and non-mercerized cotton and viscon production. The effects of residence time on chemical oxygen demand (COD), color and turbidity removals and pH change were studied under response surface optimized conditions of 30 °C, 25 g/L electrolyte concentration and 3505 mg/L COD feed concentration with 123.97 mA/cm² current density. Increasing residence time resulted in steady profiles of COD and color removals with higher treatment performances. The best column performance was realized at 3 h of residence time as 53.5% and 99.3% for COD and color removals, respectively, at the expense of 193.1 kWh/kg COD with a mass transfer coefficient of 9.47×10^{-6} m/s.

© 2009 Elsevier B.V. All rights reserved.

1. Introduction

Textile manufacturing is one of the largest industrial producers of wastewater containing processing bath residues from preparation, dyeing, finishing, slashing and other operations. These residues may cause severe pollution if not properly treated before discharge to the receiving waterways [1–3].

Dyes and auxiliary chemicals used in textile mills are improved to be resistant to environmental influences for better performance, thus it is hard to remove them from wastewater [1,2]. These chemicals generally include color residues, heavy metal ions, and electrolytes in dyeing wastewater, and toxic air emissions from discharged wastewater. Moreover, textile wastewater is well known with its high chemical oxygen demand, strong color, large amount of suspended solids, variable pH values, salt content and high temperature [4–12]. Consequently, the treatment systems combined with physical, biological and chemical methods may become insufficient for the effective treatment of industrial textile wastewater due to the variation of wastewater characteristics and heavy COD load [4–12].

In recent years, electrochemical oxidation is drawing attention as an alternative wastewater treatment method and starting to substitute traditional processes [13]. The electrochemical treatment of textile wastewater has also been studied in the literature

using cast iron, steel, Ti/RuO₂, Ti/Pt, Ti/Pt/Ir, active carbon fiber and stainless steel 304 electrodes [4–8,11,12,14,15]. However, only a few continuous electrochemical treatment studies were found in the literature. Sonoyama et al. [16] studied the continuous electrochemical decomposition of dichloromethane using a flow cell at low flow rates using Cu metal–powder column electrode. Alfafara et al. [17] treated brine wastewater with high ammonia content from an iodine processing plant by indirect electrolytic treatment process via generating chlorine at the anodes and initiating the formation of mixed oxidants like hypochlorous acid in batch and continuous modes. Sakalis et al. [18] investigated the electrochemical degradation of Reactive Orange 91, Reactive Red 184, Reactive Blue 182 and Reactive Black 5 azodyes using batch and continuous electrolytic cells with carbon fleece cathodes and Pt/Ti anodes, and sodium chloride and sodium sulfate electrolytes. Körbahti and Tanyolaç [19] studied the electrochemical treatment of phenolic wastewater in a continuous tubular reactor, constructed from a stainless steel tube with a cylindrical carbon anode at the center.

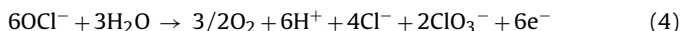
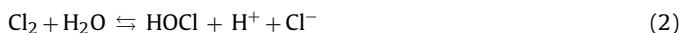
The electrochemical reactions that take place during the electrochemical treatment are rather complicated [20], and electrochemical removal mechanisms of organic pollutants are not clear. In general, organic pollutants are thought to be removed from wastewater by direct and indirect electrochemical mechanisms.

In electrochemical reactions, the presence of NaCl provides the discharge of chlorine gas in excess and in return irreversible reactions of hydrolysis and ionization occur. Immediately afterwards Cl₂ gas is discharged on the anode rapidly (reaction (1)) in the aqueous medium [20–22], hydrolysis (reaction (2)) and ionization (reaction (3)) reactions take place [21–23]. Hypochlorous acid, HOCl,

* Corresponding author. Tel.: +90 312 2977404; fax: +90 312 2992124.

E-mail addresses: korbahiti@mersin.edu.tr (B.K. Körbahti), tanyolac@hacettepe.edu.tr (A. Tanyolaç).

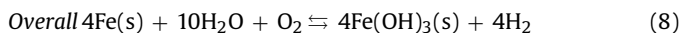
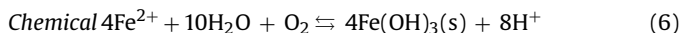
is replenished in the medium with simultaneous electrochemical reaction of NaCl in the reaction solution. HOCl is a strong oxidant, which can oxidize the wastewater while OCl^- is consumed by reaction (4) [20,24,25].



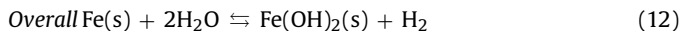
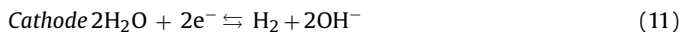
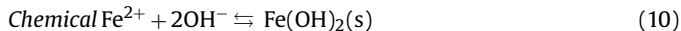
In neutral to moderate pH solutions, a cycle of chloride–chlorine–hypochlorite–chloride occurs that cause the initial concentration of chlorides to remain stable [20,25]. However, in strong alkaline solutions, the cycle of chloride–chlorine–chloride is blocked due to the production of stable ClO_3^- [20,25]. At low pH chlorides are reduced with the production of free chlorine while at high pH the chlorides are oxidized and chlorates are produced [20,25].

Moreover, with sufficient applied voltage, Fe^{+2} ions were added into the solution by the anodic reaction and some of the organic molecules and suspended solids captured by iron hydroxides. Two mechanisms for the production of iron hydroxide have been proposed in the case of iron anodes [26]:

Mechanism I:



Mechanism II:



If hydrogen gas is produced on the cathode, Fe^{n+} ions result from the oxidation of the anode can react with the OH^- ions produced at the cathode and yield insoluble iron hydroxides [26]. The insoluble iron hydroxides can remove the molecules by surface complexation or electrostatic attraction [27]. In surface complexation, it is assumed that the pollutant can act as a ligand to bind a hydrous iron portion with precipitation and adsorption mechanisms [27].

In this work, the electrochemical treatment of textile wastewater simulated from industrial components was investigated in a continuous tubular reactor with the presence of NaCl electrolyte on iron anode and stainless steel cathode for the first time in literature. The effects of residence time on treatment performance under the conditions determined previously were elucidated [28] and operational parameters were optimized with surface response methodology, RSM.

2. Materials and methods

2.1. Chemicals and electrode materials

Levafix Blue CA gran. reactive dye (DyStar), Cottoclarin F (Cognis), Belsoft 200 (Cognis), dextrin (Sigma), sucrose (Merck), hydrogen peroxide (Merck), sodium hydroxide (Merck), sodium silicate (Merck), acetic acid (Merck), sodium carbonate (Merck) and sodium chloride (Merck) were obtained in pure grade and deionized water was used for the preparation of synthetic industrial textile wastewater. All other chemicals used for the analysis were obtained

in highest degree of purity from various sources. Iron was used as the anode with 13 mm diameter, and stainless steel 6R35 (Sandvik, Sweden) was used as cathode material (cylindrical, OD = 88.9 mm and wall thickness = 2 mm) with a wt% chemical composition 0.045 C, 0.40 Si, 1.18 Mn, 0.026 P, 0.001 S, 17.45 Cr, 10.14 Ni, 0.46 Ti, and the rest Fe.

2.2. Preparation and properties of simulated industrial textile wastewater

The industrial textile wastewater was synthetically prepared based on a real process information [28,29]. The model textile process for wastewater was composed of sizing, desizing, singeing, scouring, bleaching, mercerization and dyeing of non-mercerized and mercerized cotton and viscon production. The composition and the characteristics of simulated industrial textile wastewater were presented in a previous study [28,29].

2.3. Experimental set-up and procedure

The continuous electrochemical tubular reactor was designed in our laboratory with a net working volume of 1774 cm³ [29] (Fig. 1). The 32 cm tall reactor was constructed from stainless steel with a heating/cooling coil around. The iron electrode was used as the anode material and placed at the center of the reactor. A Cole Parmer model peristaltic Masterflex[®] pump was used to pump the simulated textile wastewater from a 20 L reservoir at prescribed flow rate. The reaction temperature was controlled with circulating water recycled from a temperature controlled water bath (New Brunswick, G-86) and monitored with glass thermometers immersed in the exit and inlet of the column. The current was applied by a constant voltage/current controlled DC power source (NETES NPS-1810D).

Synthetic industrial textile wastewater with the electrolyte was prepared in the wastewater reservoir at specified concentration and was fed to the column to fill it completely. The reaction started with the application of the specified voltage/current, and the recycling water for temperature control was pumped through the reactor coil while feed stream was pumped to the column continuously. At appropriate time intervals, samples were taken from the reactor outlet and analyzed for intermediate properties of the reaction medium. DC power source was turned off and the reaction was terminated after 8 h of elapsed time.

2.4. Analysis

During the treatment 5 mL samples were taken from the electrochemical reactor at appropriate time intervals and pH was measured with a NEL pH30 model pH meter. Then the sample was centrifuged at 5000 rpm for 10 min to have supernatant for analysis and measurements. The color of the reaction medium was monitored by a Hitachi 150-20 model spectrophotometer at 595 nm and the turbidity was measured by a Hach 2100 AN IS model turbidimeter at 860 nm. COD analysis was performed with Palintest PL464 test kit after color and turbidity analysis. The samples were pre-treated in order to prevent the precipitation of Ag^+ ions in COD test kits due to Cl^- ions present in the sample [28].

2.5. Experimental design and optimization

In the study, runs were designed in accordance with D-optimal design of Design-Expert[®] 7.1 program [30,31]. The results of the runs were optimized through RSM. The independent variables; residence time and elapsed time, were coded with low and high levels in D-optimal design, while COD and color removals, pH, mass transfer coefficient and energy consumption were selected as dependent

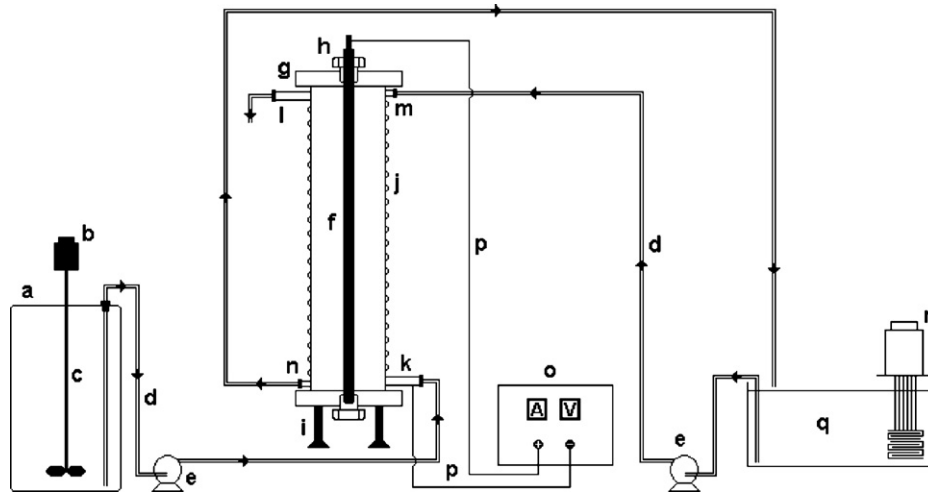


Fig. 1. The schematic view of continuous electrochemical tubular reactor (a: wastewater reservoir, b: driving motor, c: glass stirrer, d: feed lines, e: peristaltic pumps, f: electrochemical reactor, g: Plexiglas reactor cover, h: iron electrode, i: reactor support, j: heating/cooling coil, k: feed in, l: feed out, m: heating/cooling in, n: heating/cooling out, o: dc power source, p: connections, q: heating/cooling tank and r: heater).

variables, the responses. The D-optimal designed runs were augmented with three replications in order to evaluate the pure error and were carried out in randomized order as required in many design procedures.

In the optimization process, the response can be simply related to chosen factors by linear or quadratic models. A quadratic model, which also includes the linear model, is given as:

$$\eta = \beta_0 + \sum_{j=1}^k \beta_j x_j + \sum_{j=1}^k \beta_{jj} x_j^2 + \sum_{i < j=2}^k \sum_{i=1}^k \beta_{ij} x_i x_j + e_i \quad (13)$$

where η is the response, k is the number of factors, x_i and x_j are variables, β_0 is the constant coefficient, β_j 's, β_{jj} 's and β_{ij} 's are interaction coefficients of linear, quadratic and the second-order terms, respectively, and e_i is the error [30,31]. In the program, the data were processed for Eq. (13) including ANOVA to obtain the interaction between the process variables and the response. The quality of the fit of polynomial model was expressed by the coefficient of determination, R^2 and adjusted coefficient of determination, R^2_{adj} . The statistical significance was checked with adequate precision ratio, F and P values.

In the optimization, a module in Design-Expert® 7.1 software searched for a combination of factor levels that simultaneously satisfy the requirements placed on each of the responses and factors. The desired goals were selected as maximum COD and maximum color removal percents at minimum residence time and minimum energy consumption. Corresponding importances of goals were selected as 5 for COD removal and energy consumption, 3 for color removal, residence time, elapsed time and mass transfer coefficient. These individual goals were combined into an overall desirability function by Design-Expert® 7.1 software for maximization to find the best local maximum.

3. Results and discussions

Continuous tubular reactor experiments were carried out for the determination of the effects of the residence time on COD, color and turbidity removals and pH of the simulated textile wastewater as well as on mass transfer coefficient and energy consumption at optimum reaction conditions determined previously [28]. Therefore, in all continuous runs the COD feed concentration was 3505 mg/L with 25 g/L electrolyte concentration and applied current density was 123.97 mA/cm² at 30 °C reaction temperature.

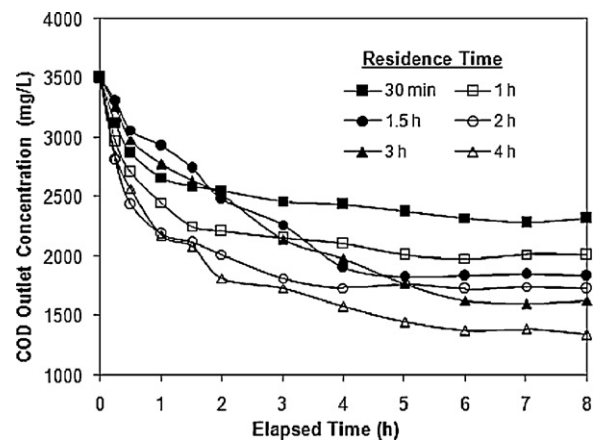


Fig. 2. The COD decrease in the tubular reactor (current density: 123.97 mA/cm²; T: 30 °C; electrolyte concentration: 25 g/L).

3.1. The effect of residence time

The discharge COD concentration, color and turbidity removals, and pH time profiles were monitored at the column reactor outlet for 30 min, 1, 1.5, 2, 3 and 4 h of residence times in Figs. 2–5.

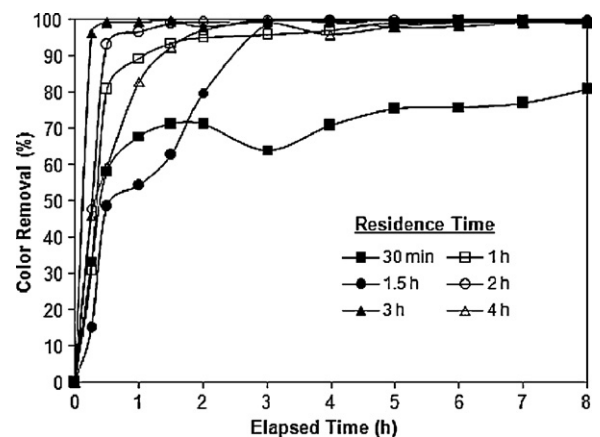


Fig. 3. The color removal in the tubular reactor (current density: 123.97 mA/cm²; T: 30 °C; electrolyte concentration: 25 g/L).

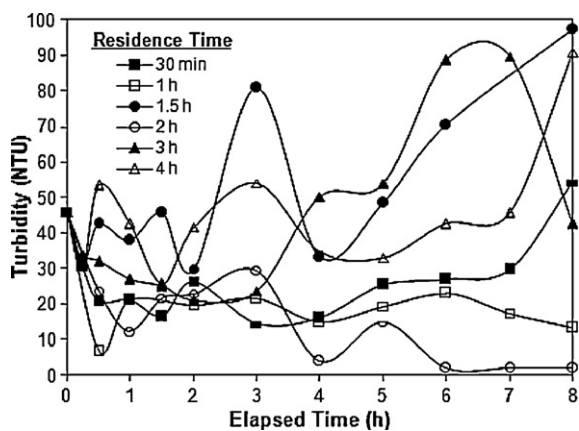


Fig. 4. The turbidity change in the tubular reactor (current density: 123.97 mA/cm²; T: 30 °C; electrolyte concentration: 25 g/L).

In Fig. 2, the steady state conditions in the tubular reactor for COD removal seemed to be established after 5 h of elapsed time. In the figure, at the end of 8 h the COD removal was realized as 34.0%, 42.7%, 47.6%, 50.6%, 53.5% and 61.7% for 30 min, 1, 1.5, 2, 3 and 4 h of residence time, respectively. Apparently, increasing residence time resulted in steady profiles of removal with higher treatment performances. In the literature, Lin and Peng [4] reached at steady state within 50 min for their continuous system using cast iron electrodes with the addition of polyaluminum chloride and realized 51% COD removal performance at 92.5 A/m² current density. Naumczyk et al. [7] obtained 85–92% COD removal after 60 min of electrolysis at 60 mA/cm² using Ti/RuO₂, Ti/Pt and Ti/Pt–Ir electrodes with an initial COD of 960 mg/L in a bench-scale batch reactor. The authors reported that chromophore groups of dyes easily degraded by direct and indirect oxidation, however, further anodic oxidation of intermediates and other organics were at much lower rate [7]. Jia et al. [8] treated simulated dyeing wastewater with 50 mg/L dye concentration using activated carbon fiber electrodes and Na₂SO₄ electrolyte in a batch reactor. They obtained 40–80% COD removal with 25 V electrolytic voltage at 60 min treating time.

The color removal at the reactor outlet for 30 min, 1, 1.5, 2, 3 and 4 h of residence time is shown in Fig. 3. After 8 h of elapsed time maximum color removal was achieved as 80.8% for 30 min of residence time and above 30 min of residence time almost complete color removal was realized. In Fig. 3, the color removal at steady state was obtained as 80.8, 98.7, 99.6, 99.6, 99.3 and 99.3 for 30 min, 1, 1.5, 2, 3 and 4 h of residence time, respectively. The rapid color removal indicates the degradation of dye into smaller

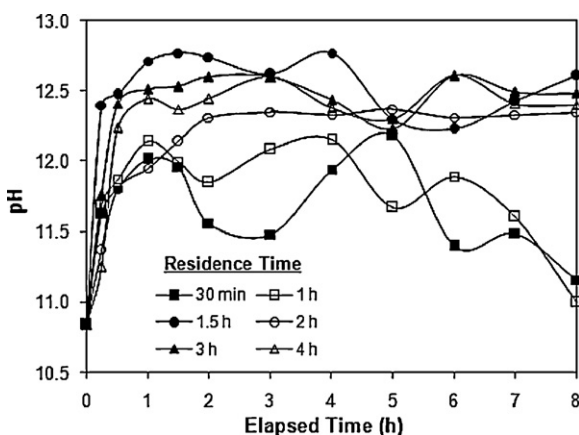


Fig. 5. The pH change in the tubular reactor (current density: 123.97 mA/cm²; T: 30 °C; electrolyte concentration: 25 g/L).

and colorless organic or inorganic products, which can further be oxidized for complete mineralization. Apparently, the rate of COD removal is lower than that of color, indicating that the azo bond degradation is the first step of the electrochemical degradation mechanism as stated in the literature [7,18,32]. As in those studies, Vlyssides et al. [12] obtained complete color removal and Naumczyk et al. [7] achieved 99% color removal after 30 min of electrolysis. Xiong et al. [15] investigated the removal of COD and color from simulated dye wastewater containing Acid Orange II with the combination of Fe(II) coagulation and electrochemical treatment with activated carbon particle electrodes, and they obtained overall color and COD removal efficiencies as 99% and 87%, respectively, under 20 V cell voltage. Shen et al. [33] found that increasing the electrolyte concentration and voltage above 3.0 V increased the color removal, where they obtained color removal between 30% and 40%. Daneshvar et al. [27] also reported that an increase in the current density up to 6–8 mA/cm² enhanced the color removal efficiency. The authors concluded that the color removal efficiency depended directly on the concentration of hydroxyl and metal ions produced on the electrodes [27]. Sakalis et al. [18] investigated the electrolytic degradation of Reactive Orange 91, Reactive Red 184, Reactive Blue 182 and Reactive Black 5 azodyes and obtained complete decoloration both using NaCl and Na₂SO₄ electrolytes for all dyes. They obtained 94.4% dye removal after real wastewater treatment under 12 V applied potential and 45% COD removal [18].

In Fig. 4, the turbidity time profiles at the reactor outlet for 30 min, 1, 1.5, 2, 3 and 4 h of residence time are shown. Only 1–3 h of residence time revealed decreased turbidity removal. It was concluded that the turbidity values fluctuated at all residence time values due to the possible formation of intermediate and complex by-products during the electrochemical treatment. In addition, the effect of residence time distribution may also cause the fluctuation in the tubular reactor. It is very well known that tubular reactors do not exhibit a true plug flow behavior always [34,35]. The flat velocity profile and no axial mixing assumptions cannot be completely used to analyze the plug flow reactors [34,35]. An ideal plug flow reactor has a fixed residence time while a real plug flow reactor has a residence time distribution that is a narrow pulse [34,35]. Therefore, residence time distribution (RTD) could be useful in explaining the fluctuation for incompressible fluids in steady state real plug flow reactors. In this study, it was concluded that the RTD of a tubular reactor deviated from an ideal reactor depending on its hydrodynamics due to fluid dispersion, non-uniform velocity profile and molecular diffusion.

Fig. 5 shows the pH time profiles at the exit of the tubular reactor. As a general trend, pH sharply increased in 30 min up to pH 11.8–12.4 from 10.8, and then fluctuated between 12.2 and 12.6 for 1.5, 2, 3 and 4 h of residence time in the tubular reactor. This increasing pH trend was observed in all runs and was most likely due to hydrolysis, ionization and OCl⁻ consumption reactions of Eqs. (2)–(4). Nevertheless, instable pH values obtained due to unestablished steady state conditions in the reactor within the time range of runs as well as non-homogeneous character of the reactor.

The experimental results were evaluated with response surface methodology of Design-Expert[®] 7.1, and the approximating functions of COD removal percent (\hat{y}_1) and color removal percent (\hat{y}_2) obtained with D-optimal design are presented in Eqs. (14) and (15), respectively. The turbidity removal was not taken into account due to its fluctuating nature.

$$\hat{y}_1 = 2.611x_1 + 12.110x_2 + 0.839x_1x_2 - 0.289x_1^2 - 1.172x_2^2 + 6.255 \quad (14)$$

$$\hat{y}_2 = 25.772x_1 + 26.142x_2 - 0.249x_1x_2 - 4.438x_1^2 - 2.501x_2^2 + 12.545 \quad (15)$$

Table 1
ANOVA results of the quadratic models for COD removal, color removal, mass transfer coefficient and energy consumption.

Source	Sum of squares	Degrees of freedom	Mean square	F-Value	P-Value
COD Removal (%)^a					
Model	17378.86	5	3475.77	79.93	<0.0001
x_1 : residence time (h)	1726.41	1	1726.41	39.70	<0.0001
x_2 : elapsed time (h)	9479.20	1	9479.20	217.99	<0.0001
x_1x_2	505.96	1	505.96	11.64	0.0011
x_1^2	8.71	1	8.71	0.20	0.6560
x_2^2	3013.29	1	3013.29	69.30	<0.0001
Residual	2869.97	66	43.48		
Color removal (%)^b					
Model	41027.48	5	8205.50	20.47	<0.0001
x_1 : residence time (h)	3679.76	1	3679.76	9.18	0.0035
x_2 : elapsed time (h)	15462.00	1	15462.00	38.57	<0.0001
x_1x_2	44.69	1	44.69	0.11	0.7395
x_1^2	2056.40	1	2056.40	5.13	0.0268
x_2^2	13723.50	1	13723.50	34.23	<0.0001
Residual	26461.26	66	400.93		
Mass transfer coefficient (m/s)^c					
Model	4.409×10^{-9}	5	8.818×10^{-10}	129.05	<0.0001
x_1 : residence time (h)	2.545×10^{-9}	1	2.545×10^{-9}	372.42	<0.0001
x_2 : elapsed time (h)	1.203×10^{-9}	1	1.203×10^{-9}	176.00	<0.0001
x_1x_2	1.828×10^{-10}	1	1.828×10^{-10}	26.75	<0.0001
x_1^2	4.988×10^{-10}	1	4.988×10^{-10}	73.01	<0.0001
x_2^2	3.327×10^{-10}	1	3.327×10^{-10}	48.69	<0.0001
Residual	4.510×10^{-10}	66	6.833×10^{-12}		
Energy consumption (kWh/kg COD removed)^d					
Model	8.862×10^5	5	1.772×10^5	193.32	<0.0001
x_1 : residence time (h)	38365.08	1	38365.08	41.85	<0.0001
x_2 : elapsed time (h)	7.870×10^5	1	7.870×10^5	858.39	<0.0001
x_1x_2	22844.18	1	22844.18	24.92	<0.0001
x_1^2	257.01	1	257.01	0.28	0.5983
x_2^2	986.66	1	986.66	1.08	0.3033
Residual	60507.42	66	916.78		

^a $R^2 = 0.86$; $R^2_{adj} = 0.85$; adequate precision = 29.11.

^b $R^2 = 0.61$; $R^2_{adj} = 0.58$; adequate precision = 15.58.

^c $R^2 = 0.91$; $R^2_{adj} = 0.90$; adequate precision = 41.49.

^d $R^2 = 0.94$; $R^2_{adj} = 0.93$; adequate precision = 44.94.

In Eqs. (14) and (15), x_1 was residence time (h) in the reactor and x_2 was elapsed time (h) during the electrolysis. ANOVA results of these quadratic models are presented in Table 1. In the table, model F -values of 79.93 and 20.47 imply the models are significant for COD and color removal percents, respectively. For both equations, adequate precision signal to noise ratio is greater than 4, which is desirable for sound models. Also for all models, P -values are less than 0.0001, indicating that terms are significant in all models while correlation coefficients denote good enough quadratic fits to navigate the design space. The normal % probability and studentized residuals graphs for responses \hat{y}_1 , \hat{y}_2 , \hat{y}_3 and \hat{y}_4 yielded fair straight lines, proving normal distribution of the data (the graphs were not shown).

Eqs. (14) and (15) have been used to visualize the effects of experimental factors on responses under optimized conditions in response surface graphs of Figs. 6 and 7. In Fig. 6, COD removal percent increased by increasing residence time and maximum COD removal was obtained at 4 h of residence time (63%) in the reactor after 6.5 h of elapsed time. However, 3 h of residence time and 5 h elapsed time are good enough for complete color removal as observed in Fig. 7.

3.2. Mass transfer coefficient

In an electrochemical reactor, mass transfer coefficient can be related to the physical parameters of the system such as electrode length, flow rate, electrode potential, and the ratio of electrode area and electrolyte volume including the solution properties [37].

However, the cell and electrode arrangements are so complex that specification of the velocity and concentration variations with time and location could not be made accurately [28,37]. Therefore, general correlations in engineering literature to express the mass transfer coefficient as Sherwood number in terms of Schmidt and

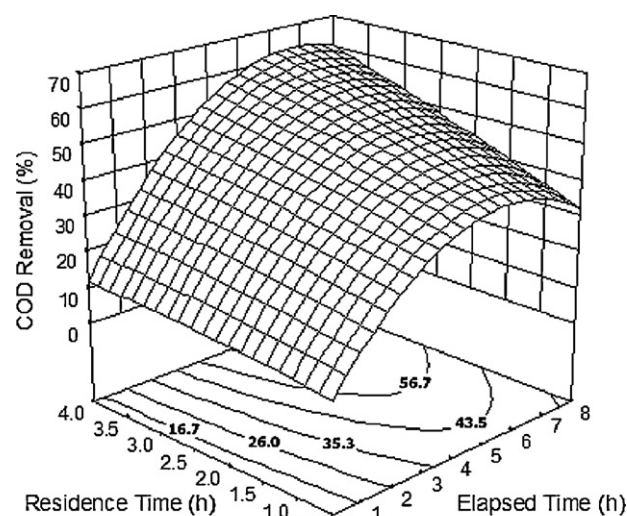


Fig. 6. The effect of residence time on COD removal (current density: 123.97 mA/cm²; T: 30 °C; electrolyte concentration: 25 g/L).

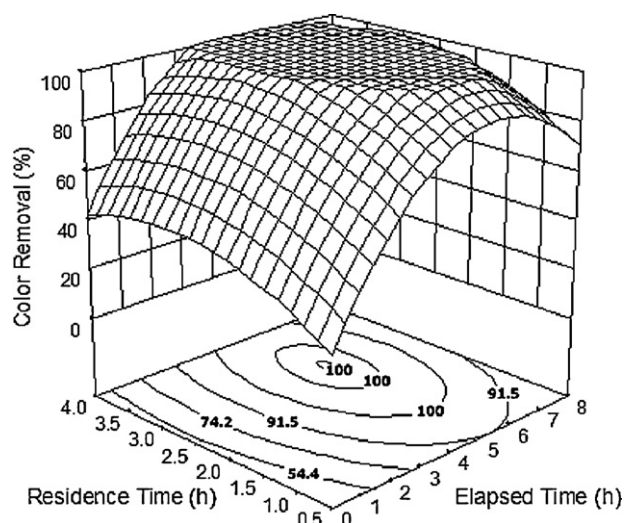


Fig. 7. The effect of residence time on color removal (current density: 123.97 mA/cm²; T: 30 °C; electrolyte concentration: 25 g/L).

Reynolds numbers may lead to unrealistic mass transfer coefficients for laminar flow [36,37].

Mass transfer coefficient for single pass plug flow reactor could be estimated by Eq. (16), which is a mass balance over the reactor via Faraday's law with the assumption that the entire electrode supports a reaction under mass transport control via convective diffusion of the reactant or product and the longitudinal dispersion of flow due to diffusion is negligible [28,37]:

$$x_{\text{PFR}} = 1 - \exp \left[\left(\frac{-k_m A}{V_R} \right) \tau_R \right] \quad (16)$$

In Eq. (16), V_R is internal reactor volume, A is the electrode area, k_m is mass transfer coefficient, τ_R is average residence time, and x_{PFR} is fractional COD conversion.

In Eq. (17), the approximating function of mass transfer coefficient (\hat{y}_3) obtained with D-optimal design is given. In Table 1, 129.05 model F value, <0.0001 P value and 41.49 adequate precision value imply that the quadratic model is significant for the mass transfer coefficient.

$$\hat{y}_3 = -1.257 \times 10^{-5} x_1 + 5.695 \times 10^{-6} x_2 - 5.041 \times 10^{-7} x_1 x_2 + 2.186 \times 10^{-6} x_1^2 - 3.895 \times 10^{-7} x_2^2 + 1.630 \times 10^{-5} \quad (17)$$

The changes of Reynolds number, k_m and fractional COD conversion with residence time in the tubular reactor are presented in Table 2. As the residence time increased, fractional COD conversion increased because of extended reaction time and Re numbers becomes smaller due to the decreased linear velocity in the reactor. The flow in the tubular reactor was in the range of 17.8×10^{-5} – 2.22×10^{-5} m/s indicating that flow regime in the column was laminar for corresponding Re num-

bers in the range $13.4 < Re < 1.7$. The mass transfer coefficient, k_m , decreased due to increasing film resistance at lower flow rates [37]. Although k_m values decreased with decreased flow rate, the increased retention time enabled higher overall mass transport to the electrodes and more reaction time for higher conversions.

In literature there are several estimated mass transfer coefficients in electrochemical treatments. Morão et al. [32] studied the electrochemical oxidation of multi-component mixtures of organic compounds using boron doped diamond anode and obtained mass transfer coefficients for phenol, phenylmethanol, 1-phenyl-ethanol and *m*-cresol degradation as 1.9×10^{-5} , 1.9×10^{-5} , 1.7×10^{-5} and 2.1×10^{-5} m/s, respectively. Panizza and Cerisola [38] investigated the electrochemical oxidation of 2-naphthol using lead dioxide, boron-doped diamond and Ti–Ru–Sn ternary oxide anodes, and determined the mass transfer coefficient in the range 0.7×10^{-5} – 2.0×10^{-5} m/s. Fernandes et al. [39] studied the electrochemical oxidation of C.I. Acid Orange 7 on a boron doped diamond electrode and calculated an average mass transfer coefficient of 1.46×10^{-5} m/s. In electrochemical reactors, mass transport processes in the liquid phase are slower than those in the gas phase [37]. Pletcher and Walsh [37] stated that this phenomenon causes much more complicated mass transport limitations on the rate of chemical changes in the reactor and the formation of reaction layers at the solid–liquid interface. In addition, the flow regime in our electrochemical reactor was laminar as seen in Table 2, which is clearly a disadvantage in mass transport of the electroactive species to the electrode surface [37]. Nevertheless, mass transfer coefficient values calculated in this study were found close to those of literature showing that our electrochemical reactor operated under mass transport control due to maximized degradation rate.

3.3. Energy consumption

The energy consumption during the electrochemical treatment of textile wastewater in the tubular reactor is given in Table 2, where E is the mean energy consumption up to stabilized conversion. The energy consumption was relatively high at low residence times due to unestablished steady state conditions and low conversion. The energy consumption decreased with increase in residence time and minimum energy consumption was obtained for 3 h of residence time as 193.1 kWh/kg COD removed in Table 2. It is also seen in Fig. 7 that an optimum point for color removal was obtained at 3 h residence time. Thus our electrochemical tubular reactor must be operated at 3 h of optimum residence time for a cost driven approach with 25 g/L electrolyte addition and 123.97 mA/cm² current density applied at 30 °C reaction temperature. These conditions ensured COD and color removals and discharge pH as 53.5%, 99.3%, and 12.5, respectively, with a prevailing mass transfer coefficient of 9.47×10^{-6} m/s.

The approximating function of energy consumption (\hat{y}_4) obtained with D-optimal design is given in Eq. (18). In Table 1, 193.32 model F value, <0.0001 P value and 44.94 adequate preci-

Table 2
The mass transfer coefficient, mass flux and energy consumption corresponding to the electrochemical treatment of simulated textile wastewater in a continuous tubular reactor (current density: 123.97 mA/cm²; T: 30 °C; electrolyte concentration: 25 g/L).

Residence time (h)	Linear velocity $\times 10^5$ (m/s)	Fractional COD conversion	Reynolds number	$k_m \times 10^{-6}$ (m/s)	E (kWh/kg COD removed)
0.5	17.8	0.340	13.37	30.8	263.7
1	8.89	0.427	6.68	20.7	297.7
1.5	5.93	0.476	4.46	16.0	241.3
2	4.44	0.506	3.34	13.1	195.8
3	2.96	0.535	2.23	9.47	193.1
4	2.22	0.617	1.67	8.91	195.3

sion value imply that the quadratic model is significant for energy consumption.

$$\hat{y}_4 = -6.415x_1 + 56.818x_2 - 5.635x_1x_2 + 1.569x_1^2 - 0.671x_2^2 + 33.418 \quad (18)$$

In literature, the mean energy consumption was determined per kg COD removed as 21 kWh [11,12], 1.273–12.3 kWh [25], 12.4 kWh [40], 4.8–200 kWh [41] and 1.273–12.3 kWh [42] for the electrochemical treatment of textile dye wastewater [11,12], olive oil wastewater [25], domestic wastewater [40], tannery waste liquors [41] and noncyanide strippers wastes [42], respectively. Productivity is favorable at high current densities; however the energy efficiency per unit amount of product decreases with the increase in cell voltage [37] as in our study. Therefore, better electrode materials and reactor configuration should be attempted before industrial applications.

3.4. Optimization of experimental conditions

The results were optimized by Design-Expert® 7.1 using the approximating functions in Eqs. (14), (15), (17) and (18). In the optimization, for a cost driven approach residence time and energy consumption were minimized within 0–8 h of elapsed time, whereas COD and color removal percents were maximized at 100% pollution load (COD = 3505 mg/L). The optimization resulted in 3 h residence time and 5 h elapsed time with the prediction of pH 12.7, 53.8% COD removal and complete color removal. Under these optimized conditions, with the desirability value of 0.578, mass transfer coefficient and energy consumption were estimated as 9.46×10^{-6} m/s and 202.4 kWh/kg COD removed, respectively. The results of the RSM optimization were in a reasonable agreement with the results obtained experimentally; only the energy consumption was overestimated with an error of 4.8%.

4. Conclusion

The electrochemical treatment of industrial textile wastewater with Levafix Blue CA reactive dye in a continuous tubular reactor constructed from a stainless steel tube with a cylindrical iron anode at the center was investigated. The effects of residence time on COD, color and turbidity removals and pH of the reaction medium were studied at 30 °C, 25 g/L electrolyte concentration and 3505 mg/L COD feed concentration with 123.97 mA/cm² current density. The required time for reaching steady state became shorter with increased residence time, which also led enhanced yield of COD and color removals. The COD and color removals were obtained as 34.0%, 80.8%; 42.7%, 98.7%; 47.6%, 99.6%; 50.6%, 99.6%; 53.5%, 99.3% and 61.7%, 99.3% for 30 min, 1, 1.5, 2, 3 and 4 h residence times, respectively. The results indicate that further advanced research should be conducted in order to improve the reaction yield and decrease the operating cost. After improvement the continuous tubular reactor could be an alternative system for the treatment of textile wastewater.

Acknowledgements

This project was supported by TUBITAK (The Scientific and Technological Research Council of Turkey) with Grant No MISAG-171. We are also very grateful to DyStar Company for supplying Levafix CA reactive dye, and Cognis Company for supplying Cottoclarin F and Belsoft 200.

References

- [1] Office of Pollution Prevention, Pollution prevention studies in the textile wet processing industry, Virginia, 1995.
- [2] U.S. Environmental Protection Agency, Best management practices for pollution prevention in the textile industry, EPA625R96004, USA, 1996.
- [3] U.S. Environmental Protection Agency, EPA Office of Compliance Sector Notebook Project: Profile of the textile industry, EPA310R97009, USA, 1997.
- [4] S.H. Lin, C.F. Peng, Treatment of textile wastewater by electrochemical method, *Water Res.* 28 (1994) 277–282.
- [5] S.H. Lin, C.F. Peng, Continuous treatment of textile wastewater by combined coagulation, electrochemical oxidation and activated sludge, *Water Res.* 30 (1996) 587–592.
- [6] S.H. Lin, M.L. Chen, Textile wastewater treatment by enhanced electrochemical method and ion exchange, *Environ. Technol.* 18 (1997) 739–746.
- [7] J. Naumczyk, L. Szpyrkowicz, F. Zilio-Grandi, Electrochemical treatment of textile wastewater, *Water Sci. Technol.* 34 (1996) 17–24.
- [8] J. Jia, J. Yang, J. Liao, W. Wang, Z. Wang, Treatment of dyeing wastewater with ACF electrodes, *Water Sci. Technol.* 33 (1999) 881–884.
- [9] X.Z. Li, Y.G. Zhao, Advanced treatment of dyeing wastewater for reuse, *Water Sci. Technol.* 39 (1999) 249–255.
- [10] R. Pelegrini, P. Peralta-Zamora, A.R. de Andrade, J. Reyes, N. Durán, Electrochemically assisted photocatalytic degradation of reactive dyes, *Appl. Catal. B Environ.* 22 (1999) 83–90.
- [11] A.G. Vlyssides, M. Loizidou, P.K. Karlis, A.A. Zorpas, D. Papaioannou, Electrochemical oxidation of a textile dye wastewater using a Pt/Ti electrode, *J. Hazard. Mater.* B70 (1999) 41–52.
- [12] A.G. Vlyssides, D. Papaioannou, M. Loizidou, P.K. Karlis, A.A. Zorpas, Testing an electrochemical method for treatment of textile dye wastewater, *Waste Manage.* 20 (2000) 569–574.
- [13] C. Pulgarin, N. Adler, P. Péringier, Ch. Comminellis, Electrochemical detoxification of a 1,4-benzoquinone solution in wastewater treatment, *Water Res.* 28 (1994) 887–893.
- [14] L. Szpyrkowicz, C. Juzzolino, S.N. Kaul, A comparative study on oxidation of disperse dyes by electrochemical process, ozone, hypochlorite and Fenton Reagent, *Water Res.* 35 (2001) 2129–2136.
- [15] Y. Xiong, P.J. Strunk, H. Xia, X. Zhu, H.T. Karlsson, Treatment of dye wastewater containing acid orange II using a cell with three-phase three-dimensional electrode, *Water Res.* 35 (2001) 4226–4230.
- [16] N. Sonoyama, K. Ezaki, T. Sakata, Continuous electrochemical decomposition of dichloromethane in aqueous solution using various column electrodes, *Adv. Environ. Res.* 6 (2001) 1–8.
- [17] C.G. Alfafara, T. Kawamori, N. Nomura, M. Kiuchi, M. Matsumura, Electrolytic removal of ammonia from brine wastewater: scale-up, operation and pilot-scale evaluation, *J. Chem. Technol. Biotechnol.* 79 (2004) 291–298.
- [18] A. Sakalis, K. Mpoulmpasakos, U. Nickel, K. Fytianos, A. Voulgaropoulos, Evaluation of a novel electrochemical pilot plant process for azodyes removal from textile wastewater, *Chem. Eng. J.* 111 (2005) 63–70.
- [19] B.K. Körbahti, A. Tanyolaç, Continuous electrochemical treatment of phenolic wastewater, *Water Res.* 37 (2003) 1505–1514.
- [20] A.G. Vlyssides, C.J. Israillides, M. Loizidou, G. Karvouni, V. Mourafetti, Electrochemical treatment of vinasse from beet molasses, *Water Sci. Technol.* 36 (1997) 271–278.
- [21] J.S. Do, W.C. Yeh, Paired electrooxidative degradation of phenol with *in situ* electrogenerated hydrogen peroxide and hypochlorite, *J. Appl. Electrochem.* 26 (1996) 673–678.
- [22] S.H. Lin, C.T. Shyu, M.C. Sun, Saline wastewater treatment by electrochemical method, *Water Res.* 32 (1998) 1059–1066.
- [23] G. Tchobanoglous, F.L. Burton (Eds.), *Wastewater Engineering, Metcalf & Eddy, Inc.*, McGraw-Hill Inc., Singapore, 1991.
- [24] Ch. Comminellis, A. Nerini, Anodic oxidation of phenol in the presence of NaCl for wastewater treatment, *J. Appl. Electrochem.* 25 (1995) 23–28.
- [25] C.J. Israillides, A.G. Vlyssides, V.N. Mourafetti, G. Karvouni, Olive oil wastewater treatment with the use of an electrolysis system, *Bioresour. Technol.* 61 (1997) 163–170.
- [26] K. Rajeshwar, J.G. Ibanez, *Environmental Electrochemistry*, Academic Press, USA, 1996.
- [27] N. Daneshvar, A. Oladegaragoze, N. Djafarzadeh, Decolorization of basic dye solutions by electrocoagulation: an investigation of the effect of operational parameters, *J. Hazard. Mater.* B129 (2006) 116–122.
- [28] B.K. Körbahti, A. Tanyolaç, Electrochemical treatment of simulated textile wastewater with industrial components and Levafix Blue CA reactive dye: optimization through response surface methodology, *J. Hazard. Mater.* 151 (2008) 422–431.
- [29] B.K. Körbahti, System design and process development for electrochemical treatment of industrial water-based paint wastewater and textile wastewater, PhD Dissertation, Hacettepe University, Ankara-Turkey, 2003.
- [30] D.C. Montgomery, *Design and Analysis of Experiments*, fourth ed., John Wiley & Sons, USA, 1996.
- [31] R.H. Myers, D.C. Montgomery, *Response Surface Methodology: Process and Product Optimization Using Designed Experiments*, second ed., John Wiley & Sons, USA, 2002.

- [32] A. Morão, A. Lopes, M.T. Pessoa de Amorim, I.C. Gonçalves, Degradation of mixtures of phenols using boron doped diamond electrodes for wastewater treatment, *Electrochim. Acta* 49 (2004) 1587–1595.
- [33] Z.M. Shen, D. Wu, J. Yang, T. Yuan, W.H. Wang, J.P. Jia, Methods to improve electrochemical treatment effect of dye wastewater, *J. Hazard. Mater.* B131 (2006) 90–97.
- [34] H.S. Fogler, *Elements of Chemical Reaction Engineering*, second ed., Prentice Hall International Editions, USA, 1992.
- [35] O. Levenspiel, *Chemical Reaction Engineering*, third ed., John Wiley & Sons, USA, 1999.
- [36] M.I. Ismail, *Electrochemical Reactors: Their Science and Technology*, Part A, Elsevier, The Netherlands, 1989.
- [37] D. Pletcher, F.C. Walsh, *Industrial Electrochemistry*, Chapman and Hall, USA, 1990.
- [38] M. Panizza, G. Cerisola, Influence of anode material on the electrochemical oxidation of 2-naphthol Part 2. Bulk electrolysis experiments, *Electrochim. Acta* 49 (2004) 3221–3226.
- [39] A. Fernandes, A. Morão, M. Magrinho, A. Lopes, I. Gonçalves, Electrochemical degradation of C. I. Acid Orange 7, *Dyes Pigments* 61 (2004) 287–296.
- [40] A.G. Vlyssides, P.K. Karlis, N. Rori, A.A. Zorpas, Electrochemical treatment in relation to pH of domestic wastewater using Ti/Pt electrodes, *J. Hazard. Mater.* B95 (2002) 215–226.
- [41] A.G. Vlyssides, C.J. Israilides, Detoxification of tannery waste liquors with an electrolysis system, *Environ. Pollut.* 97 (1997) 147–152.
- [42] A.G. Vlyssides, P.K. Karlis, A.A. Zorpas, Electrochemical oxidation of noncyanide strippers wastes, *Environ. Int.* 25 (1999) 663–670.